WACQT | Wallenberg Centre for Quantum Technology

OpenSuperQ

Control-Signal Crosstalk in Flip-Chip Superconducting Quantum Processors

Sandoko Kosen (Chalmers University of Technology)

CHALMERS Team

Tahereh Abad
Anuj Aggarwal
Janka Biznárová
Liangyu Chen
Miroslav Dobsicek
Jorge Fernández-Pendás
Simon Pettersson Fors
Göran Johansson
Sandoko Kosen
Christian Križan
Hang-Xi Li
Eleftherios Moschandreou
Andreas Nylander
Amr Osman
Robert Rehammar
Marcus Rommel
Anita Fadavi Roudsari
Daryoush Shiri
Tom Vethaak
Christopher Warren
Alexey Zadorozhko
Anton Frisk Kockum
Giovanna Tancredi
Per Delsing
Jonas Bylander

VTT Team

Marco Caputo
Leif Grönberg
Kestutis Grigoras
Joonas Govenius

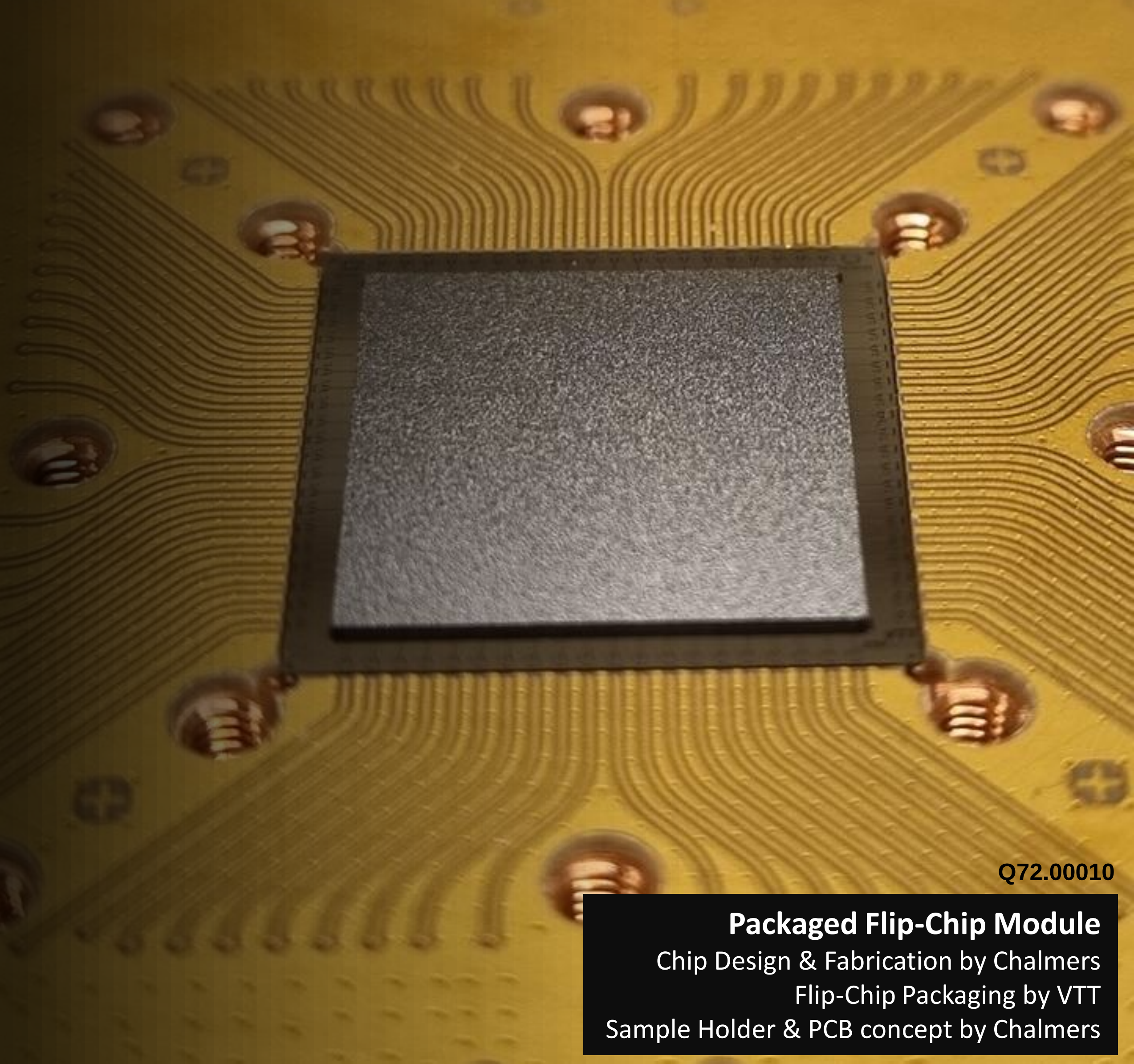

Q72.00010

Packaged Flip-Chip Module
Chip Design & Fabrication by Chalmers
Flip-Chip Packaging by VTT
Sample Holder & PCB concept by Chalmers

1st generation flip-chip processors with a scalable layout and routing strategy

Basic elements

Looking at the Q-chip

Fixed-frequency transmon coupled to four frequency-tunable couplers

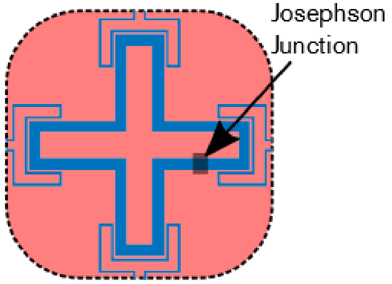

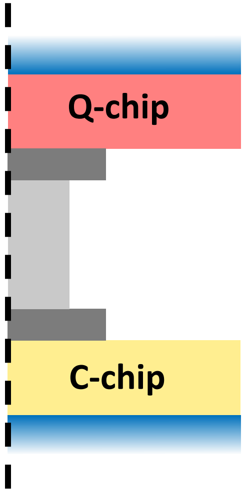

Looking at the C-chip, through the Q-chip

XY-line and readout resonator opposite the qubit.

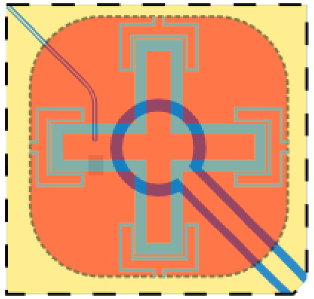

Z-line opposite a structure with SQUID

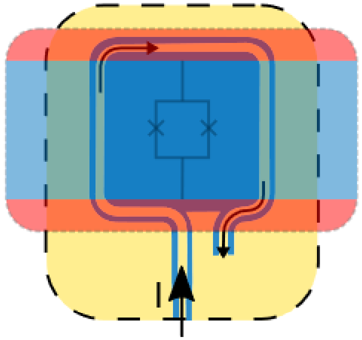

Routing corridor between two qubit rows

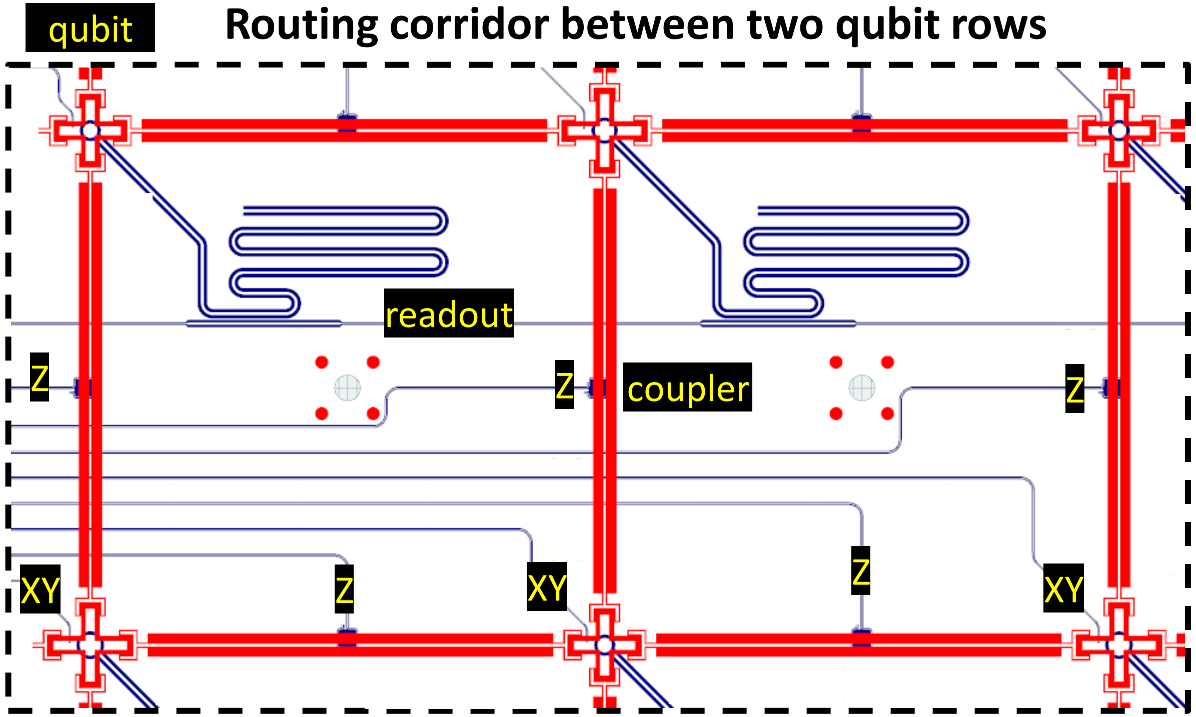

Automation of design and simulation

Qiskit | quantum device design

Ansys

Chalmers code

1.1 General properties of quantum measurements

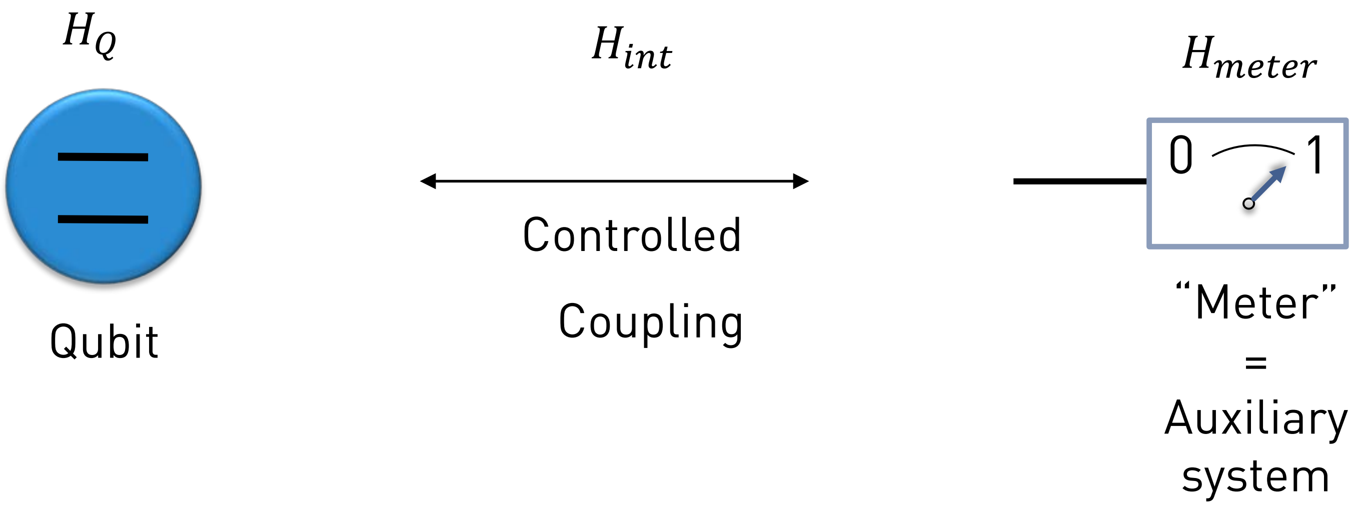

Desirable properties:

- Projective and Quantum non-demolition (QND)
  - Coupling to the meter does not change the state of the qubit $[H_Q, H_{int}] = 0$.
  - Repeated measurement yields the same outcome.
- Good ON/OFF ratio
  - $[H_{int}\,, H_{meter}] = 0$ during "OFF"
  - $[H_{int}\,, H_{meter}] \neq 0$ during "ON"
- No spontaneous decay/excitation due to measurement apparatus
- Fast and high fidelity

1.2 Circuit QED

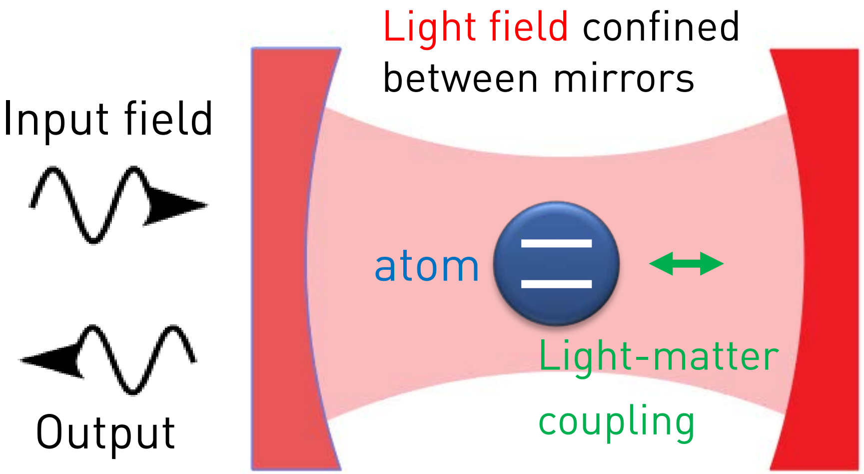

Circuit ⟷ equivalent

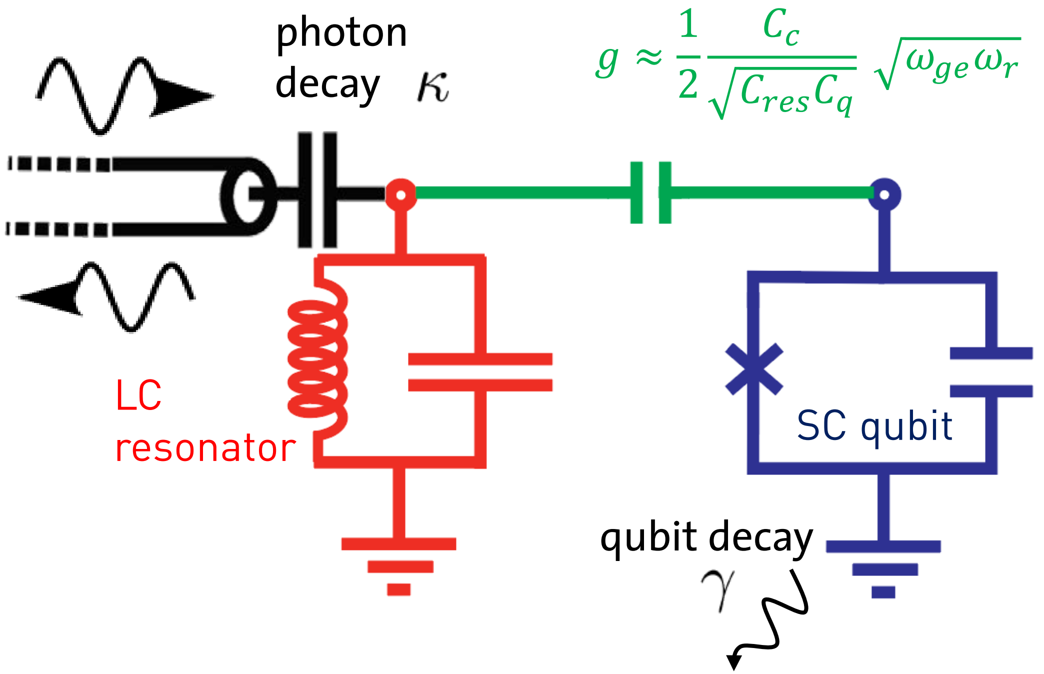

System Hamiltonian (compare chapter 2):

$$H_{\mathrm{sys}}/\hbar = \omega_r a^\dagger a \quad + \quad \omega_{ge} b^\dagger b - \frac{\alpha}{2}(b^\dagger)^2 b^2 \quad - \quad g(a - a^\dagger)(b - b^\dagger)$$

$$= \boxed{\omega_r a^\dagger a} + \boxed{\frac{\omega_{ge}}{2}\sigma^z} \boxed{+ g(a^\dagger \sigma^- + a\sigma^+)}$$

Resonator field — qubit — coupling

Jaynes-Cummings Hamiltonian

- Rotating wave approximation (RWA)
- Two-level approximation

S. Haroche & J. Raimond, Exploring the Quantum, OUP Oxford (2006)

1.3 Circuit QED: Resonant case and dispersive limit

Jaynes-Cummings Hamiltonian:

$$H/\hbar = \underbrace{\boxed{\omega_r a^\dagger a}}_{\text{quantized field}} + \underbrace{\boxed{\frac{\omega_{ge}}{2}\sigma^z}}_{\text{qubit}} + \underbrace{\boxed{g(a^\dagger\sigma^- + a\sigma^+)}}_{\text{coupling}}$$

Strong coupling regime: $g > \gamma,\ \kappa$

What happens in the limit of large detuning?

$$|\Delta| = |\omega_{ge} - \omega_r| \gg g$$

$$\boxed{\chi\sigma_z a^\dagger a}$$

Dispersive coupling

- Limit of large detuning is referred to as the dispersive limit. No resonant exchange of excitations.
- In the dispersive regime coupling Hamiltonian commutes with qubit Hamiltonian.

Energy level diagram for resonant case $\omega_r = \omega_{ge}$:

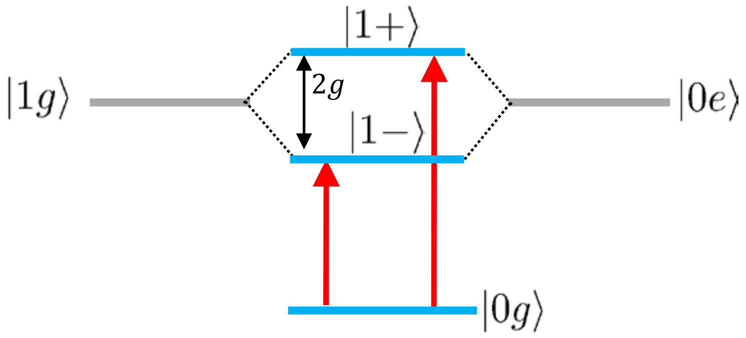

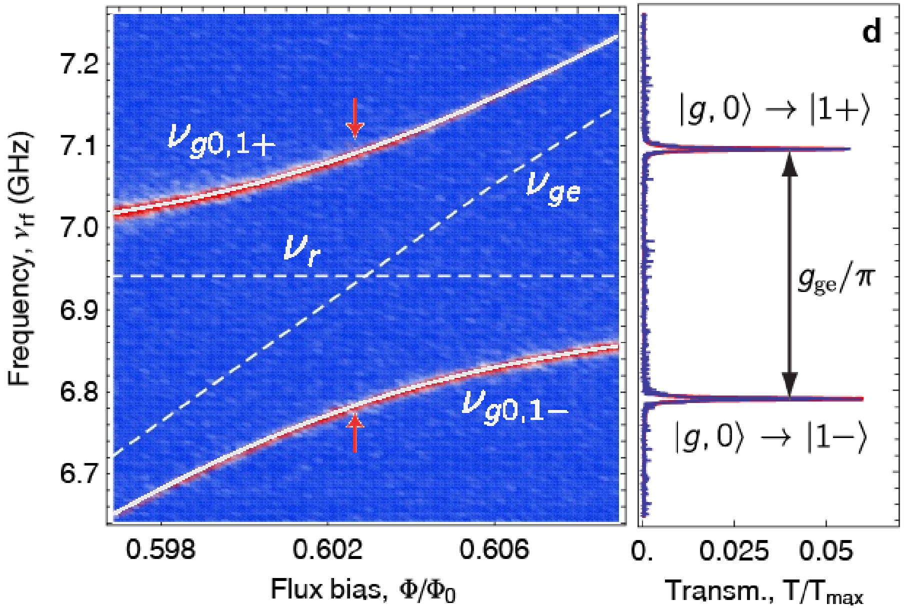

A. Wallraff *et al.*, *Nature* 431, 162 (2004), J. Fink et al., Nature (London) 454, 315 (2008)

1.4 Principle of Dispersive Qubit Measurement

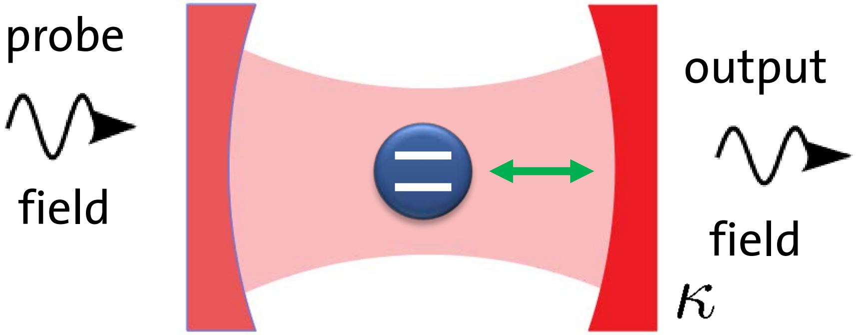

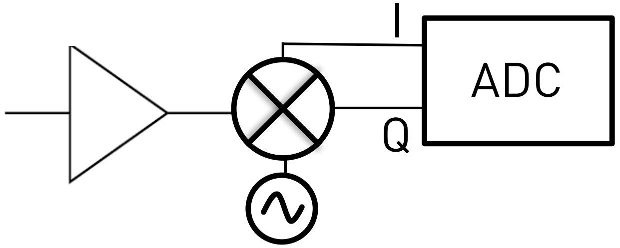

$$A\, e^{i\phi} = I + i\, Q$$

signal amplitude

Phase

In-phase and quadrature components

In the limit of large detuning $\omega_\mathrm{r} - \omega_{ge} \gg g$:

$$H/\hbar \approx (\omega_\mathrm{r} + \chi\sigma_z)a^\dagger a$$,with $\chi \approx -\alpha \frac{g^2}{\Delta(\Delta-\alpha)}$

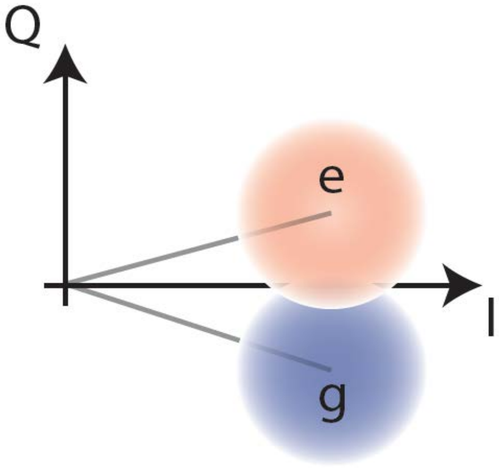

Amplitude of transmitted signal:

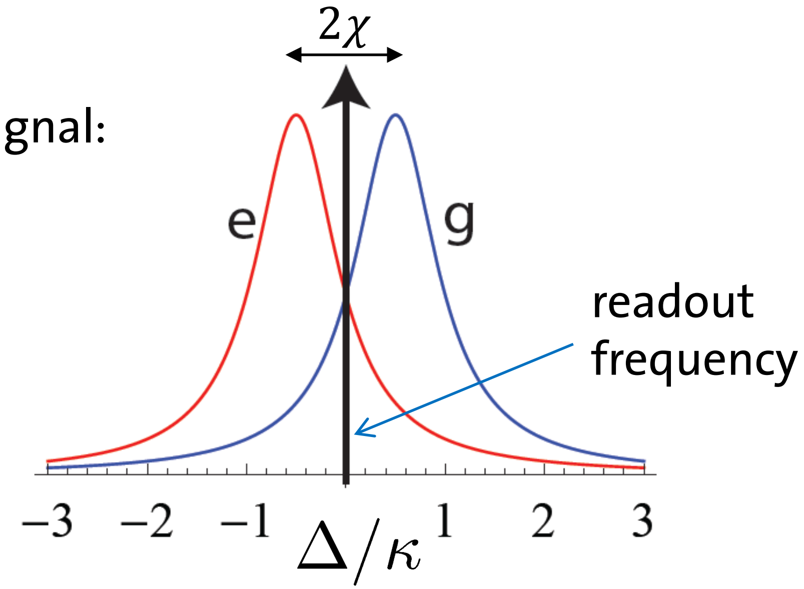

A. Wallraff *et al., Phys. Rev. Lett.* 95, 060501 (2005).
R. Vijay *et al., Phys. Rev. Lett.* 106, 110502 (2011).

1.5 Readout Resonator Response

Transmission amplitude or readout resonator extracted through Purcell filter for qubit prepared in ground (g) or excited (e) state :

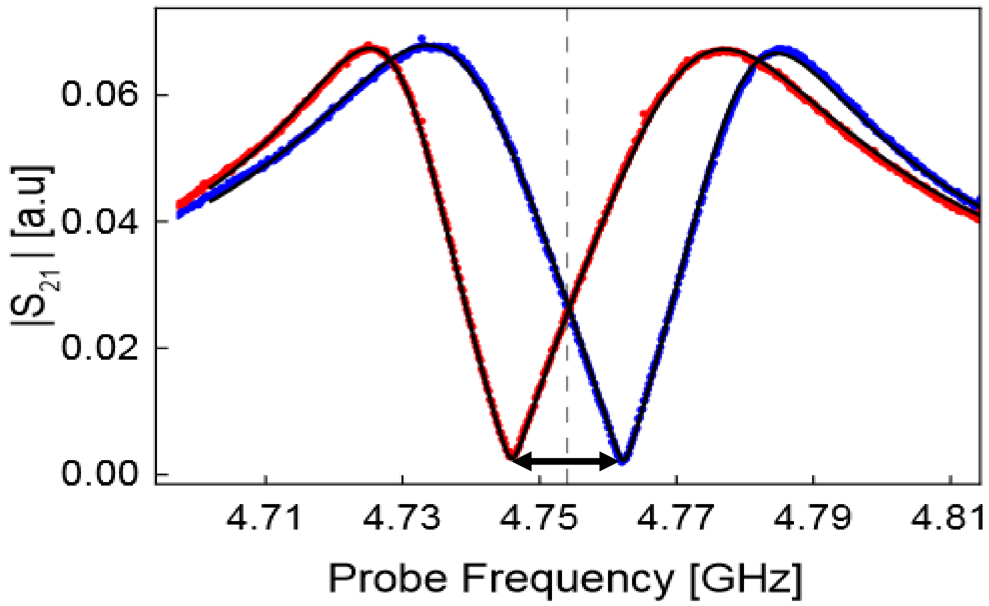

Parameter fit (input-output model):

Readout resonator $\kappa_r/2\pi$ = 37.5 MHz

State dependent resonator shift $2\chi/2\pi \simeq$ -16 MHz

In ground/excited state:

Data measured after state prep. (*,*)

Fit to resonator response model (-)

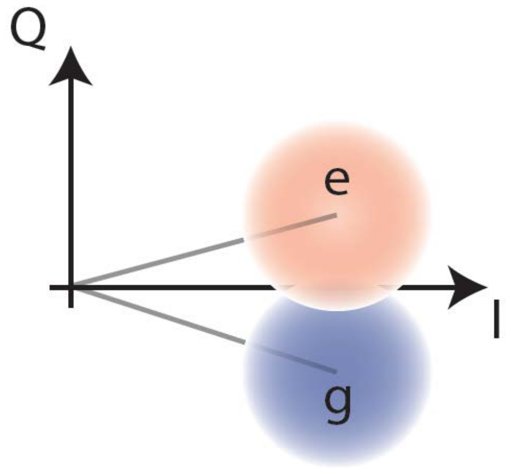

Walter et al., *Phys. Rev. Applied* **7**, 054020 (2017)

2.1 Control and Characterization of superconducting qubits

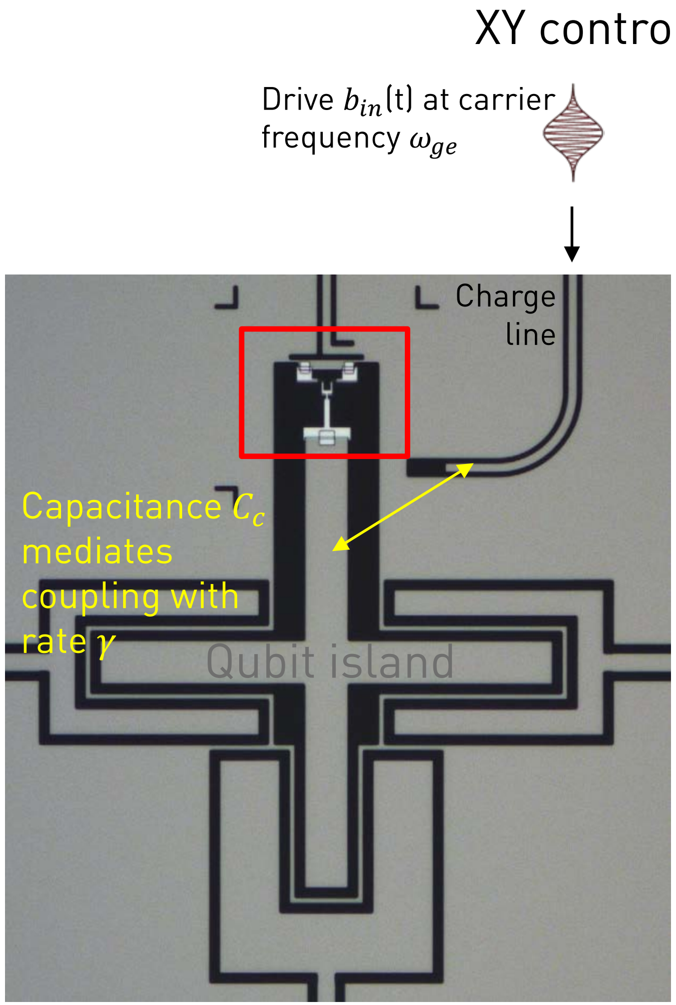

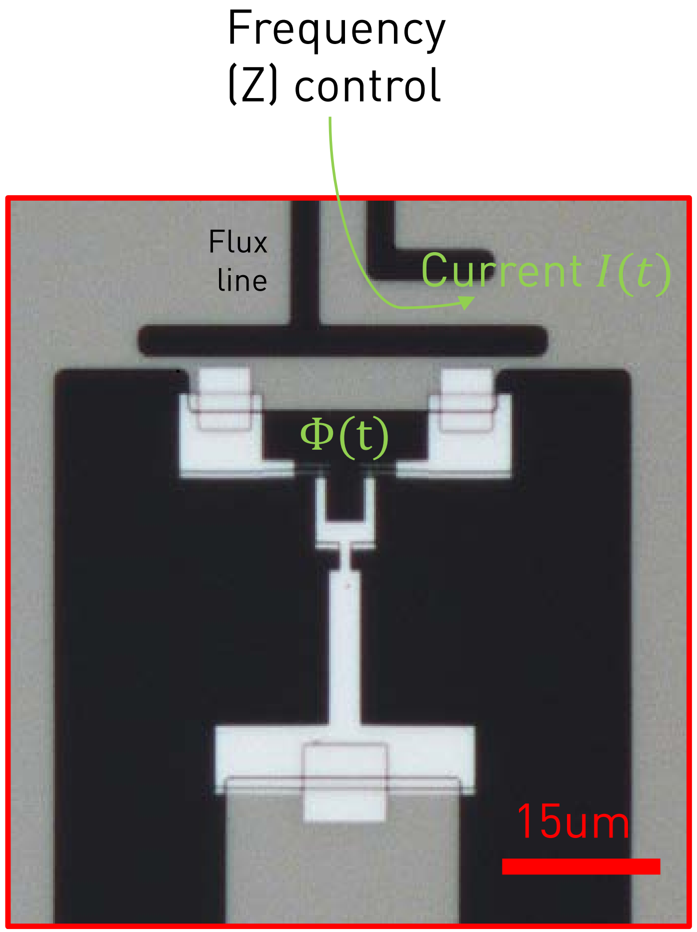

On-chip control

- Microwave drive b_{in}(t) resonant with qubit frequency rotates Bloch vector about X and Y axis. Drive power $P_{in} = \hbar\omega b_{in}^{+} b_{in}$.
- Arbitrary waveform generators (AWG) used to generate pulses, up-converted to the MW frequency band by mixing with a local oscillator field.
- Coupling rate to charge line $\gamma = \frac{C_c^2 Z_0 \omega^2}{C_\Sigma}$ imposes decay and therefore needs to be $\gamma \ll 1/T_1$.
- Tunability of the qubit achieved by sending a current $I(t)$ to a separate control line generating a magnetic flux $\Phi(t)$in the SQUID loop.
- Used for both static (DC) control of the qubit frequency and for applying pulses on nanosecond timescales.

2.1 Control and Characterization of superconducting qubits

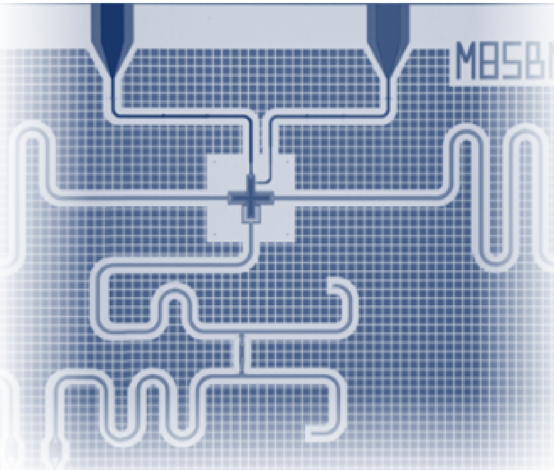

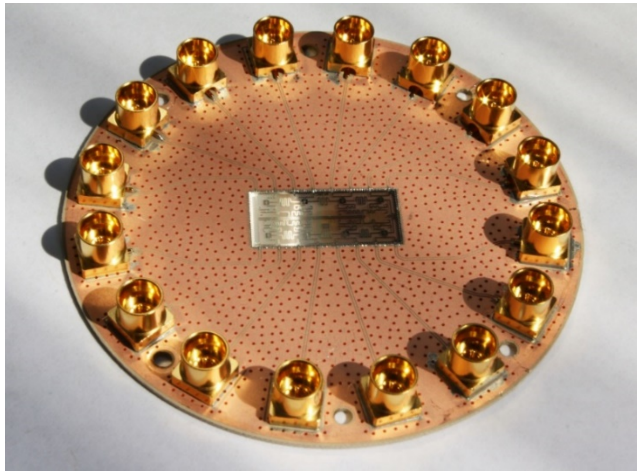

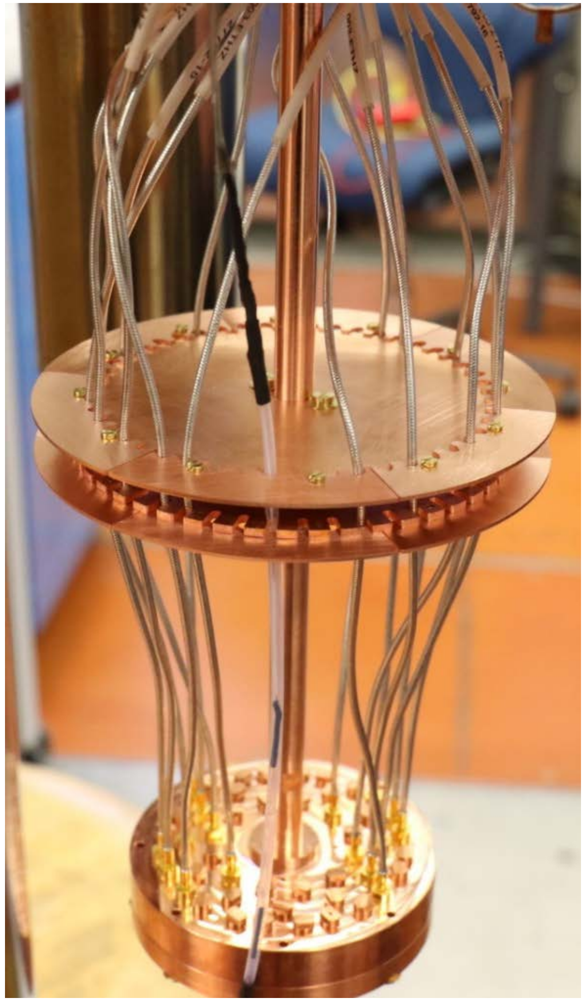

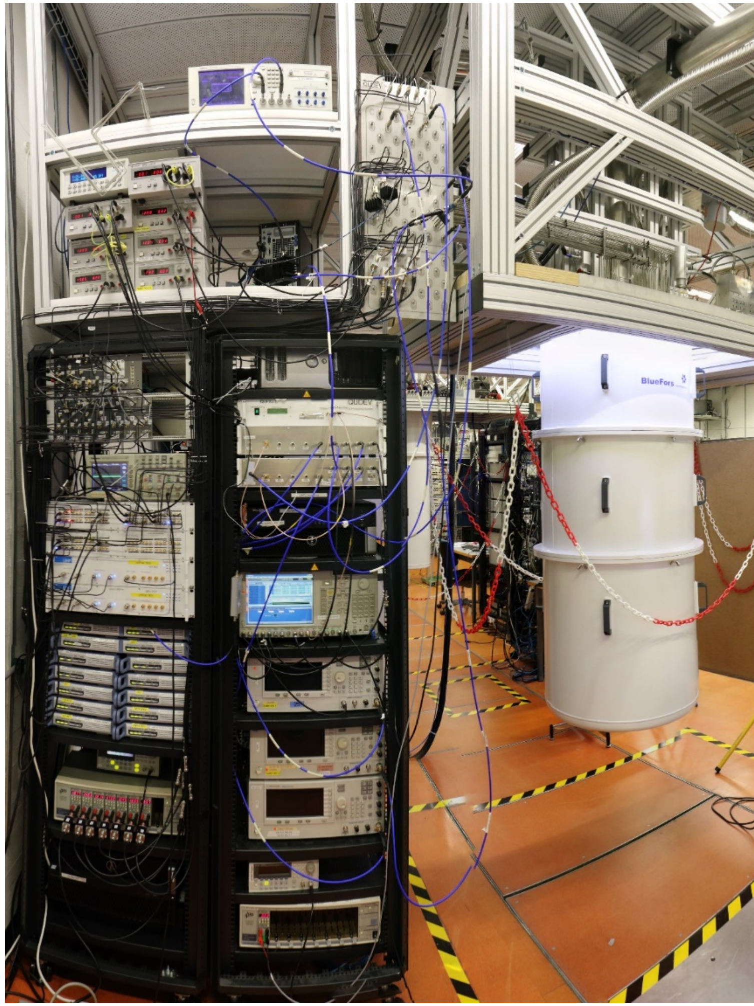

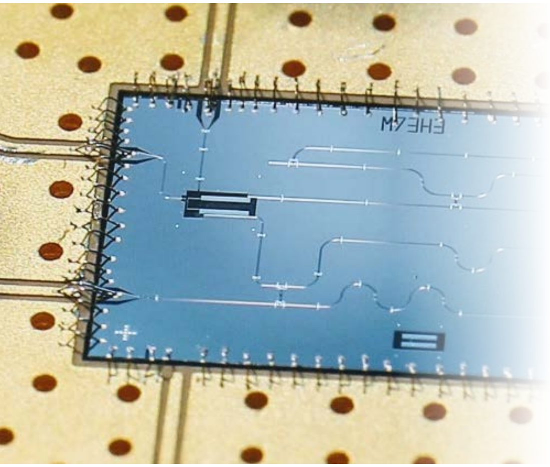

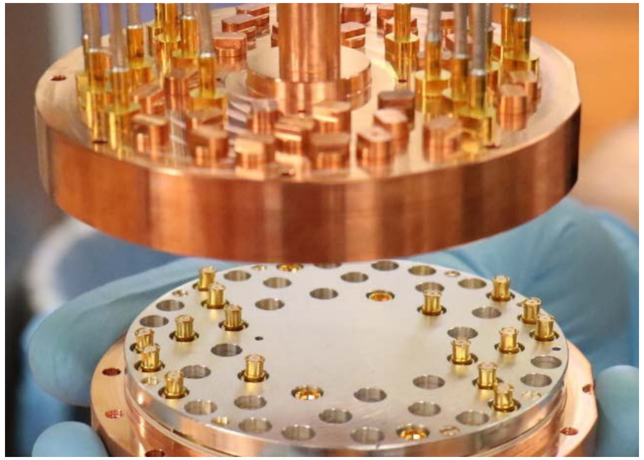

2.2 Measurement of Rabi oscillations

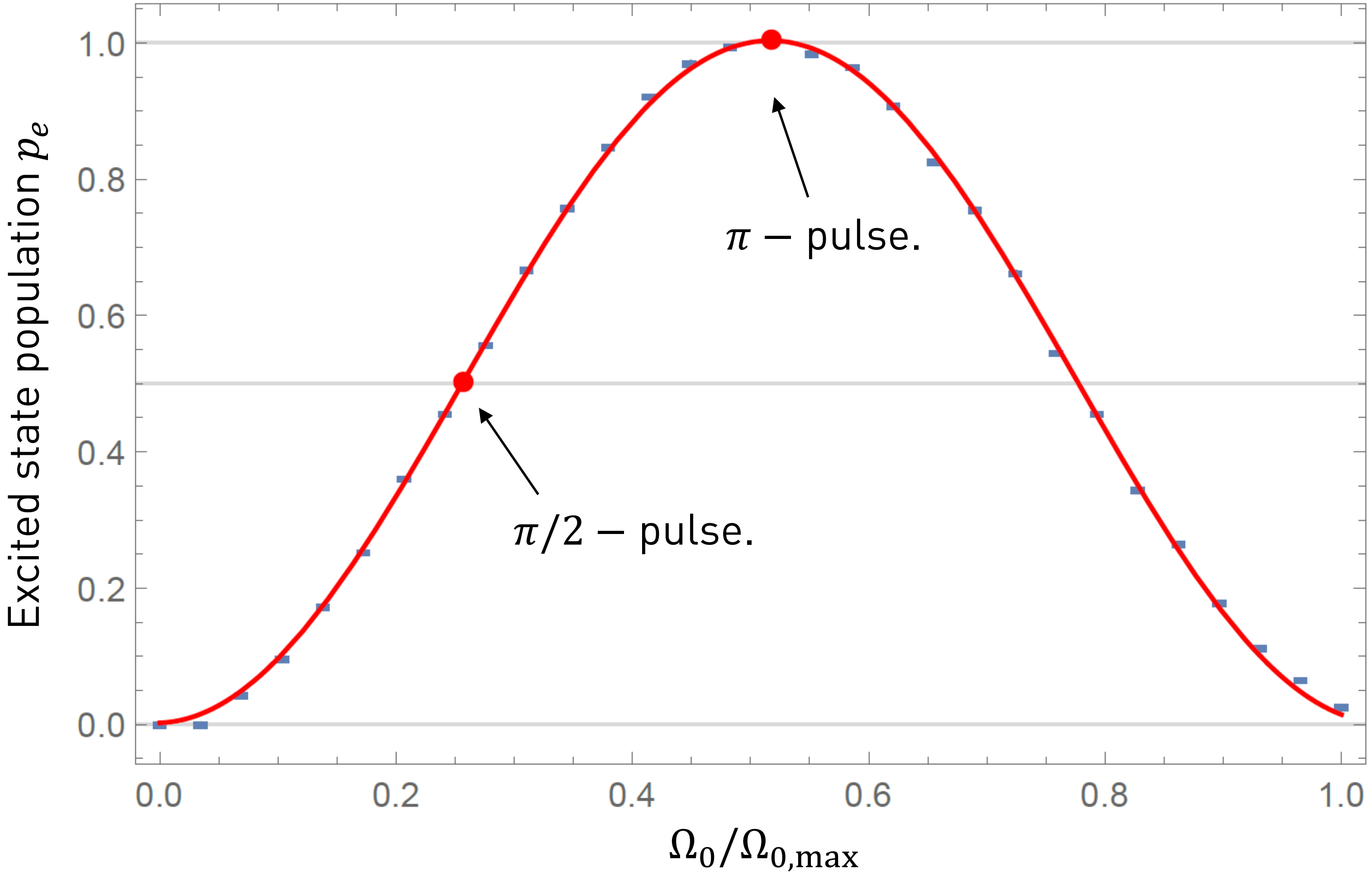

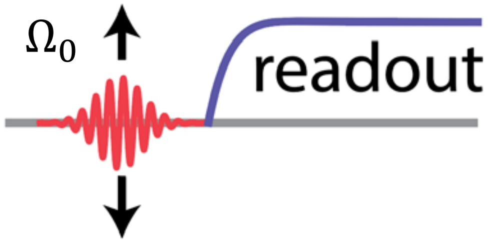

- Qubit frequency $\omega_{ge}/2\pi\ =\ 5.758\ \text{GHz}$ determined spectroscopically.
- Initialize qubit in ground state.
- Apply pulse at ω_{ge} with variable amplitude Ω_0.
- Gaussian pulse envelop with characteristic $\sigma \sim 5 - 10ns$.
- Readout qubit state and average over ~10^3 repetitions.
- Sinusoidal fit to extract π- and $\pi/2$-pulse amplitude.

2.3 Measurement of dephasing time

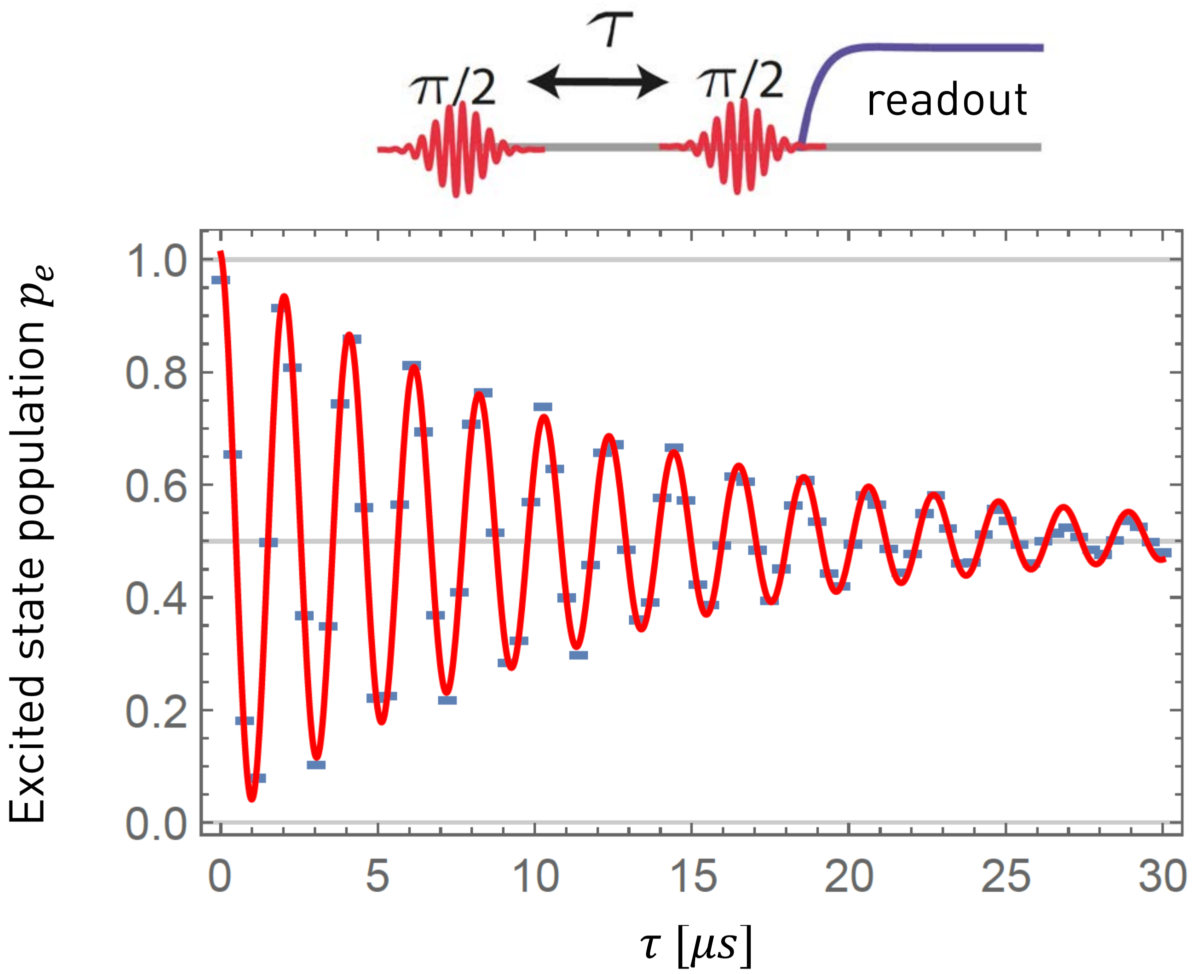

- Initial $\frac{\pi}{2}$ -pulse prepares $|g\rangle + |e\rangle$.
- Map remaining coherence after time τ to excited state using a second $\frac{\pi}{2}$- pulse, and measure.
- Detune pulse by $\mathrm{f_{IF}} = 0.5\ \mathrm{MHz}$ from qubit frequency to obtain oscillating pattern. → Higher accuracy in estimating the qubit frequency.
- Fit Characteristic decay time $T_2^* = 13\ \mu s$
- In this case, decay reasonably well described by exponential function $e^{-\tau/T_2^*}$
- Depending on spectral properties of the dominant noise source, decay better described by different functional form, e.g. Gaussian decay for 1/f – noise.
- If relaxation is only source of decoherence: $T_2 = 2\,T_1$ ("T1 limit of dephasing time").

Ithier, G. et al. PRB 72, 134519 (2005).

2.3 Measurement of dephasing time

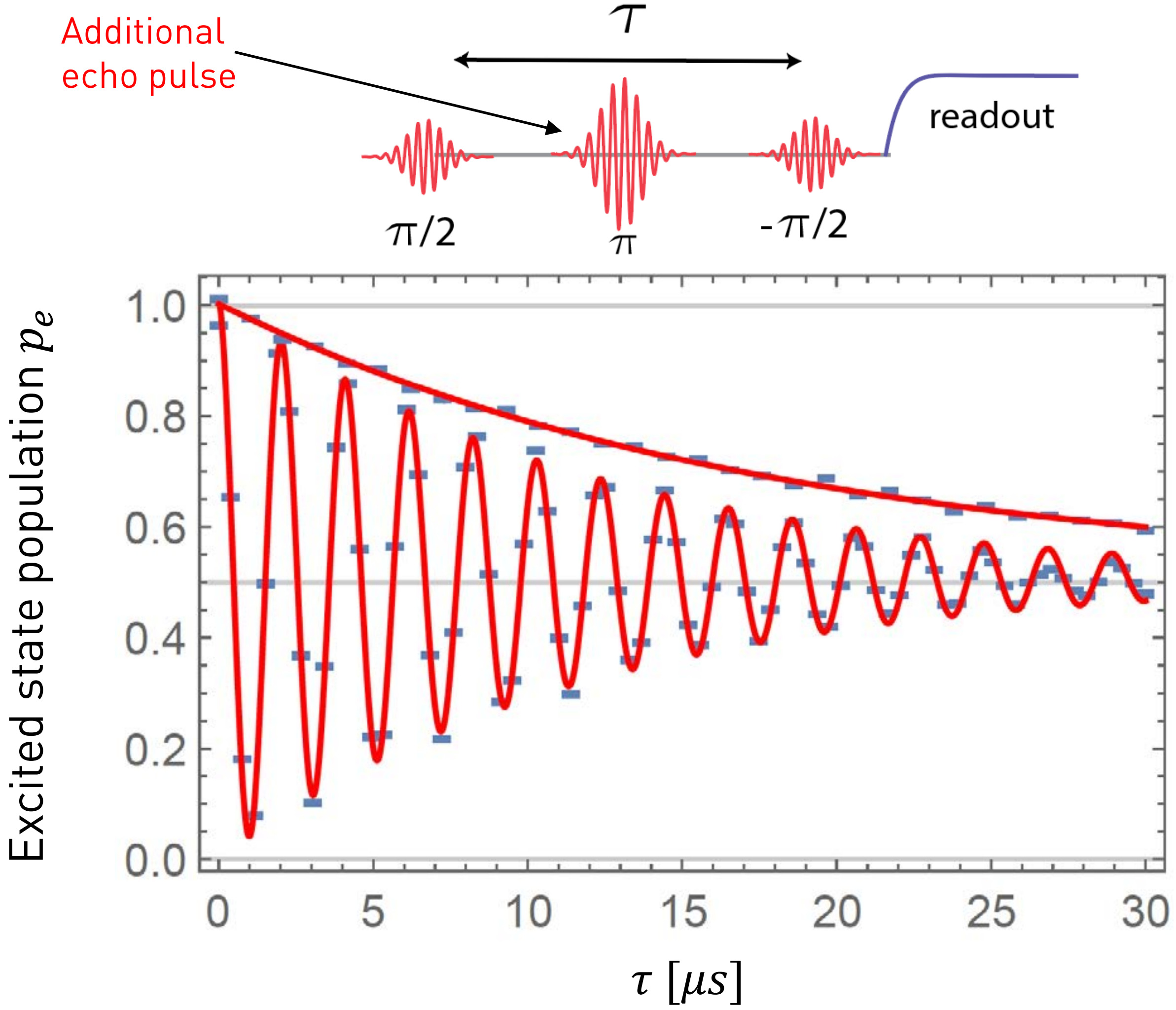

- Low frequency noise can be partly compensated for by applying an echo π-pulse after $\tau/2$ to reverse the direction of the Lamor precision.
- The resulting decay time $T_2^{echo} = 18\ \mu s$ is longer than T_2^*.
- Explanation: Low frequency noise which causes the qubit frequency to change on timescales longer than τ_{max} will cancel out.
- Variants of such dynamical decoupling sequences can be used to do noise spectroscopy → See e.g*. Bylander et al., Nat. Phys. (2011)*

Ithier, G. et al. PRB 72, 134519 (2005).

3.1 Characterization & Benchmarking of Quantum Processes

Ideally

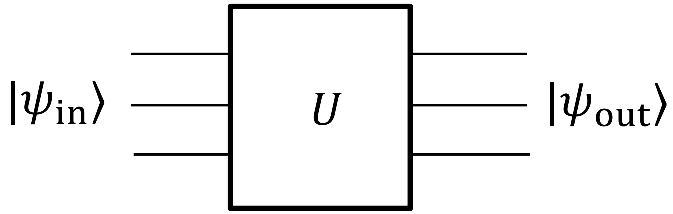

Realistically

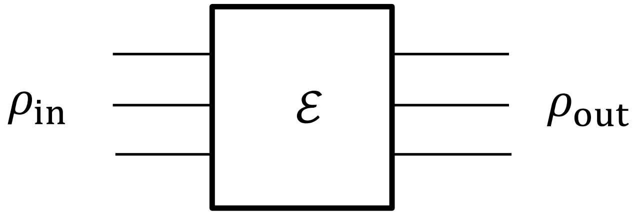

Questions:

- General properties of the map $\mathcal{E}$?
- How to measure the map $\mathcal{E}$?
  - State and process tomography
- Measure of distance between quantum states and processes: Fidelity
- How to benchmark quantum gates with fidelities close to one?
  - Randomized Benchmarking

3.2 Randomized benchmarking

- For simplicity, consider single-qubit case.
- Apply sequence of n gate operations U_i before measuring.

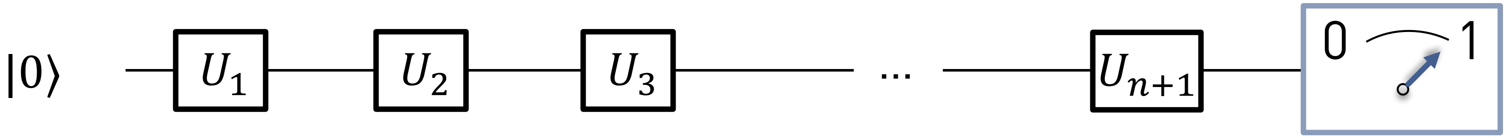

- Gates U_i are chosen randomly from the Clifford group, mapping an element of the Pauli group to an element of the Pauli group. For a single qubit there are 24 Clifford gates.
- Last gate U_{n+1} is chosen such that in the absence of errors state is brought back to initial state, i.e. $U_{n+1} \dots U_2 U_1 = I$.
- Average over m different such sequences.
- Success probability p_0 to recover the initial state decays exponentially with # of gates $p_0 \propto \alpha^n$, with depolarization parameter α.
- The error per gate is given by $\epsilon_{RB} = (1-\alpha)\frac{(d-1)}{d}$ where d is the dimension of Hilbert space (d=2 for a single qubit).

Knill et al., PRA **77**, 012307 2008

3.3 Randomized benchmarking: Example single qubit gates

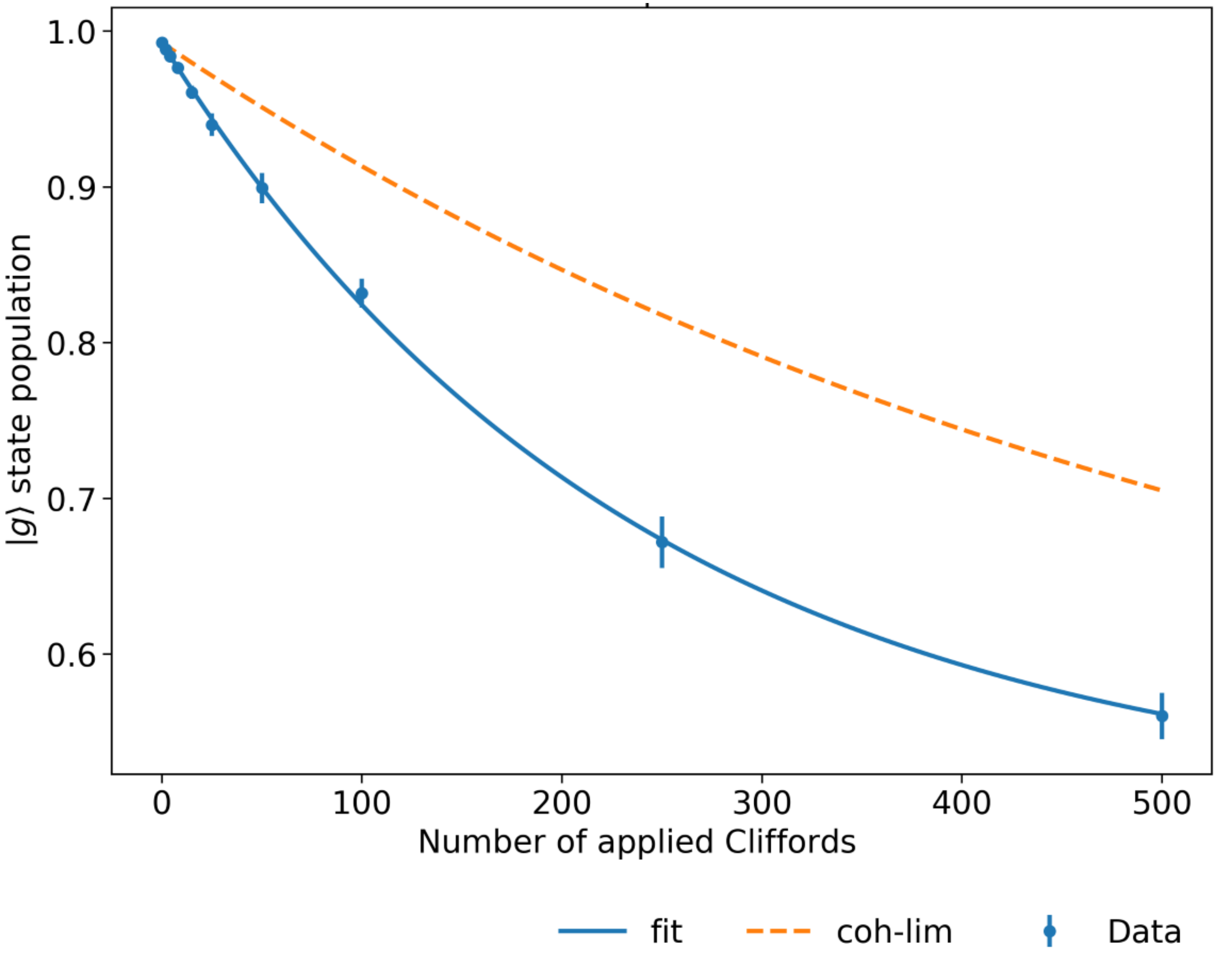

- Pulse duration typically between 15 to 50 ns. Leakage into second excited state avoided by using (DRAG*) pulse parametrization.
- Use Clifford decomposition in terms of X rotations and virtual Z gates (see McKay et al., PRA (2017)).
- Population of ground state decays exponentially.
- Fitted depolarization parameter $\alpha \approx 99.6\%$ and gate error $\epsilon \approx 0.2\%$ in this example.
- Orange dashed line indicates the limit expected when only considering qubit decoherence.
- Deviation from coherence limit hints at finite control errors, e.g. resulting in leakage to the f-level.

*Motzoi et al., PRL 103, 110501 (2009)

3.4 Interleaved Randomized benchmarking (IRB)

Question how to characterize the fidelity of one particular Clifford gate V?

- Compare decay of standard RB sequence …

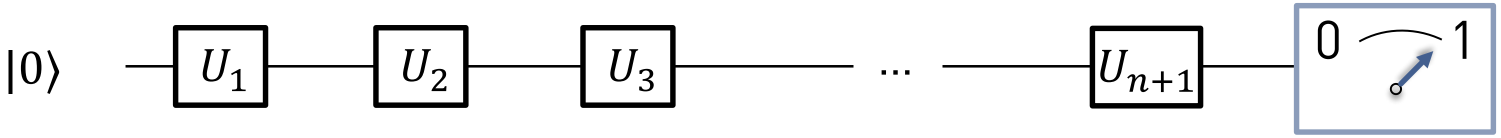

- …with result of a 2nd experiment, in which gate V gets interleaved with random Clifford gates.

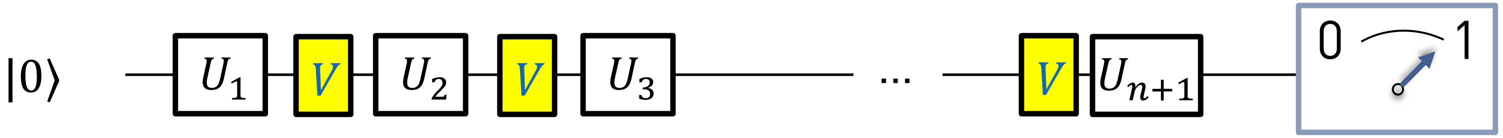

- Difference between the depolarization parameters α_{RB} and α_{IRB} results in an estimate for the error $\epsilon_V = \frac{d}{d+1}(1 - \frac{\alpha_{IRB}}{\alpha_{RB}})$ per gate V.

- Randomized Benchmarking can be generalized to multi-qubit gates.

Magesan et al., PRL 109, 080505 (2012)